Journal of ELECTRONIC MATERIALS, Vol. 47, No. 1, 2018
DOI: 10.1007/s11664-017-5786-0

Growth of Interfacial Intermetallic Compound Layer in Diffusion-Bonded SAC–Cu Solder Joints During Different Types of Thermomechanical Excursion

ANWESHA KANJILAL[1] and PRAVEEN KUMAR[1,2]

1.—Department of Materials Engineering, Indian Institute of Science, Bangalore 560012, India.
2.—e-mail: praveenk@materials.iisc.ernet.in

The effects of mechanical strain on the growth kinetics of interfacial intermetallic compounds (IMCs) sandwiched between Cu substrate and Sn-1.0 wt.%Ag-0.5 wt.%Cu (SAC105) solder have been investigated. Isothermal aging (IA) at 70°C and 125°C, and thermal cycling (TC) as well as thermomechanical cycling (TMC) with shear strain of 12.8% per cycle between −25°C and 125°C were applied to diffusion-bonded solder joints to study the growth behavior of the interfacial IMC layer under various types of thermomechanical excursion (TME). The microstructure of the solder joint tested under each TME was observed at regular intervals. It was observed that the growth rate of the IMC layer was higher in the case of TMC compared with TC or IA. This increased growth rate of the IMC layer in the presence of mechanical strain suggests an additional driving force that enhances the growth kinetics of the IMC. Finite element analysis was performed to gain insight into the effect of TC and TMC on the stress field in the solder joint, especially near the interface between the solder and the substrate. Finally, an analytical model was developed to quantify the effect of strain on the effective diffusivity and express the growth kinetics for all three types of TME using a single expression.

Key words: Effective diffusivity, interfacial intermetallic compounds, solder joints, strain-enhanced IMC growth, thermomechanical excursion

INTRODUCTION

Due to the increasing complexity of microelectronic devices, designing reliable package-level interconnection systems has become critical. Electronic devices consist of various components, and one of the weakest links in them, often being blamed for their failure, is the solder joint. Quite often, excessive growth of the interfacial intermetallic compound (IMC) layer, which forms during fabrication of solder joints as Sn from solder reacts with Cu, Ni, and other metallizations in the bond pad and grows during service via solid-state diffusion and reaction, is responsible for such failures. This is primarily because the interfacial IMC layer is the most brittle component of a solder joint, also being susceptible to void nucleation (e.g., Kirkendall voids[1–3]) and crack growth.[4] Therefore, it is important to study the evolution of the thickness of the interfacial IMC layer to ascertain the reliability of solder joints.

During reflow, molten solder reacts with the Cu substrate, forming a layer of Cu_6Sn_5 IMC at the interface. A layer of Cu_3Sn may also form between this Cu_6Sn_5 IMC layer and the Cu substrate predominately by reaction between Cu_6Sn_5 and Cu, especially at temperatures above 80°C or after longer aging times.[1,3,5] Interestingly, the IMC layer, especially the Cu_6Sn_5 phase, continues to thicken even during room-temperature storage[6,7] in the solder joints fabricated using low-melting Sn-based

(Received January 14, 2017; accepted September 1, 2017; published online September 19, 2017)

SAC solders with melting temperature of ~223°C to 226°C,[8–10] depending on their composition. The kinetic parameters for the growth of the interfacial IMC layer can be obtained by plotting the variation of its thickness, h, versus time in the case of isothermal aging, according to the following power-law equation:

$$h = h_0 + A_0 t^n \exp\left(-\frac{\Delta H}{RT}\right), \quad (1)$$

where h_0 is the initial IMC thickness, A_0 is the preexponential diffusion factor, n is the time exponent for growth (equal to 0.5 and 1 for diffusion- and reaction-controlled growth, respectively[3]), ΔH is the activation energy for growth of the interfacial IMC, R is the universal gas constant, and T is absolute temperature. There is a general consensus that growth of Cu-Sn IMCs at the solder–Cu interface is diffusion controlled,[1–3] with activation energy in the range from 40 kJ/mol to 85 kJ/mol.[1–3]

Following decades of study on the growth kinetics of the interfacial IMC layer in Sn-rich solder joints on Cu substrates using various types of sample configuration and different types of isothermal aging conditions, the mechanism of IMC growth and the different parameters in Eq. 1 are now well established. However, this field of research is still far from maturity, especially for the following two reasons: (1) solder joints undergo thermomechanical loading, wherein significant cyclic strain is imposed on the joint during service, and (2) the so-called infinite reservoir of Sn is not readily available in the miniaturized solder joints after a certain time, hence continuous formation of Cu_6Sn_5 IMC through reaction of Cu and Sn or Cu_3Sn and Sn is no longer possible in these joints, so this particular IMC may not thicken monotonically with continued aging. Equation 1 does not consider these two possibilities, hence a modification in its form is warranted to capture the true growth kinetics of the interfacial IMC layer. This study aims to modify Eq. 1 by considering the effect of cyclic strain on the growth behavior of the IMC layer, under the condition of sufficient supply of Sn in the joint, proffering continued formation of Cu_6Sn_5. Below, we elaborate more on the need for such study.

Different components that are connected by solder joints may have widely different coefficients of thermal expansion (CTEs).[4] Therefore, a change in the temperature of a device, and in particular of the solder joints, possibly reaching 165°C during regular service,[2,4] causes differential thermal expansion and hence significant straining of the solder joints. Repeated heating–cooling due to the on–off cycle of a microelectronic device will therefore impose cyclic loading on the solder joints. Interestingly, it has been shown that such thermomechanical cycling (TMC) significantly enhances the growth of Ag_3Sn and Cu_6Sn_5 precipitates in bulk solders.[7,11] Furthermore, although conflicting, there are reports suggesting a noticeable effect of static loading on the growth kinetics of the interfacial IMC in solder joints.[1,2] However, limited studies have been carried out on the effect of TMC on the growth behavior of the interfacial IMC layer. In this context, the only known study was performed by the authors of this work, where the effect of thermal cycling (TC), isothermal aging (IA), and TMC on the growth of the interfacial IMC layer was studied using reflowed solder joints.[12] In that preliminary study,[12] it was reported that the growth behavior of the interfacial IMC layer could be noticeably enhanced upon application of strain. However, due to the scallop morphology of the interfacial IMC layer in reflowed solder joints, the diffusion and hence growth behavior of the IMC layer may be multidimensional, making it extremely challenging to perform meaningful analysis or modeling. Interestingly, this problem could be overcome by forming diffusion-bonded solder joints, where the initial IMC layer formed is thin and uniform. Accordingly, this work uses such diffusion-bonded solder joints between Sn-1.0 wt.%Ag-0.5 wt.%Cu (SAC105) and Cu to reveal and quantify the role of strain in the growth behavior of the interfacial IMC layer. Finite element analysis (FEA) was also used to map the stress field near the solder–substrate interface, and a closed-form analytical model was developed to incorporate cyclic strain into Eq. 1 in order to predict the IMC thickness under different types of thermomechanical excursion (TME).

EXPERIMENTAL PROCEDURES AND NUMERICAL ANALYSIS

Experimental Procedures

To fabricate solder joints using a diffusion couple process, small rectangular coupons of SAC105 solder with cross-sectional area of 6 mm × 6 mm and thickness of 1.5 mm were first prepared by rolling solder bars. Cu blocks, also with cross-sectional area of 6 mm × 6 mm, were cut using wire electrical discharge machining. Subsequently, the rolled solder coupons and Cu blocks were metallographically polished to 3-μm of diamond so that the surfaces became flat and smooth to ensure proper contact between the surfaces of the adjacent components in the joint. Subsequently, the thin solder coupon was sandwiched between two Cu blocks, and the assembly was then held using a cast-iron C-clamp with sufficiently high pressure (~50 MPa) to enable diffusion bonding. Finally, the assembly was kept inside a furnace at 130°C for 72 h to form the diffusion-bonded solder joint. At this temperature, Sn from the solder and Cu from the substrate are known to react in solid state to form an IMC layer, primarily comprising Cu_6Sn_5, at the interface.[13,14] This interfacial IMC formation enabled good metallurgical bonding between the solder and substrate.

Once a solder joint was fabricated, it was cut into two halves along their vertical line of symmetry

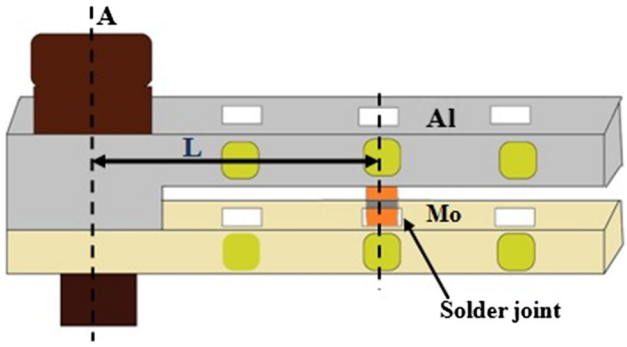

Fig. 1. Bimetallic fixture with Al and Mo arms used to impose shear strain on the solder joint during TMC. There were three slots in the fixture; depending on the distance from point A, different strains could be imposed on the joint. It was assumed that all the differential displacement was accommodated by the solder only.

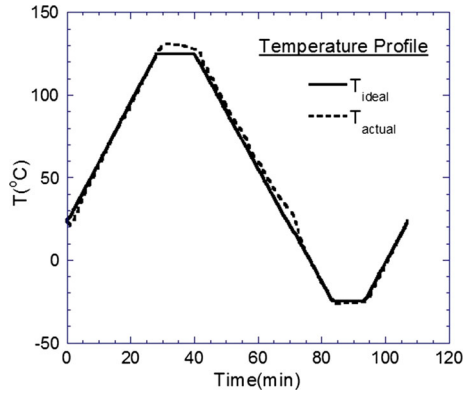

Fig. 2. Temperature profile of thermal cycle profile used for TC and TMC thermal excursion. T_{ideal} and T_{actual} are the temperature profile programmed into the environmental chamber and the actual temperature profile measured at the solder joint, respectively. The match between T_{ideal} and T_{actual} is reasonable, hence T_{ideal} was used for calculations in this study.

using a slow-speed diamond cutter. This enabled observation of the cross-section of the joint, where there was proper bonding between the solder and Cu, in contrast to the edges. The joints were then polished to 0.04-μm colloidal silica finish, then observed under scanning electron microscope (SEM) using backscattered electrons (BSE), and the initial thickness of the interfacial IMC layer was measured. Use of BSE improved the contrast between various phases of the solder joints (e.g., Cu, solder, Cu_6Sn_5, and Cu_3Sn), as these phases have different effective masses. Once the initial microstructure was recorded, the solder joints were subjected to one of the following three types of TME:

1. Thermal cycling (TC) between −25°C and 125°C up to 350 cycles, with an interruption after every 50 cycles for inspection of the microstructure
2. Thermomechanical cycling (TMC) with imposed shear strain of ~12.8% per cycle between −25°C and 125°C up to 350 cycles, with an interruption after every 50 cycles for inspection of the microstructure
3. Isothermal aging (IA) at 70°C and 125°C for 50 h, with investigation of IMC growth at regular intervals.

As shown in Fig. 1, a bimetallic fixture comprising Al (CTE, $\alpha = 23 \times 10^{-6}$/K) and Mo ($\alpha = 4.8 \times 10^{-6}$/K)[15] was used to apply the shear strain onto the solder joints during TMC. Due to the significant difference in CTE between Al and Mo, a shear strain, γ, was imposed onto the joints. The magnitude of γ can be given as

$$\gamma = \frac{L\Delta\alpha\Delta T}{h}, \quad (2)$$

where L is the distance from the fixed end of the bimetallic fixture to the center of the solder joint (i.e., the distance to the neutral point; see Fig. 1).

A typical thermal cycle, used for both TC and TMC, consisted of four segments, as described below and shown in Fig. 2:

1. Increasing temperature from −25°C to 125°C at ramp rate of 3.5°C/min
2. Holding at 125°C for 15 min
3. Decreasing temperature from 125°C to −25°C at rate of 3.5°C/min
4. Holding at −25°C for 10 min.

As mentioned above, after every 50 cycles of TC or TMC and after regular intervals of IA, the tests were interrupted to monitor the growth of the interfacial IMC as well as any flaw nucleation in the joint. After interruption, all samples were metallographically polished to 0.04-μm colloidal silica, during which material was removed to depth of 2 μm, then the microstructure was observed at the same location as earlier. The locations in the solder joint were identified based on the distance from each end of the joint. The IMC thickness, h, was analyzed using ImageJ software. As shown in Fig. 3, ImageJ software allows boundaries to be applied in a micrograph based on the inherent contrast of the image (see the thin black line surrounding the IMC layer in Fig. 3). Once such area demarcation was performed satisfactorily, the effective thickness of the interfacial IMC layer was calculated by dividing the integrated area, A_i, by the width of the micrograph (i.e., L_1). This way of measuring IMC thickness was cross-verified by manually measuring the thickness using the square-grid method. Note that an attempt was not made to distinguish between Cu_6Sn_5 and Cu_3Sn phases in the interfacial IMC layer, the reason for which is explained below in "Growth of Interfacial IMC Layer" section.

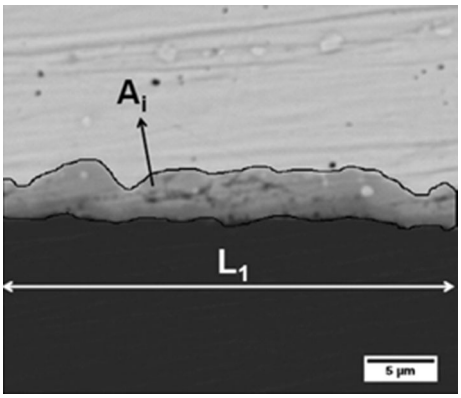

Fig. 3. Illustration of method employed using ImageJ software to measure the average thickness of the interfacial IMC layer. The solid dark curve in the center of the image shows the boundary across the interfacial IMC layer. Area A_i was divided by the width of the micrograph L_1 to estimate the average thickness of the interfacial IMC layer.

Finite Element Analysis

Two-dimensional (2-D) FEA using ANSYS® software was performed to gain insight into the stress distribution in the solder joint during TC and TMC types of TME. To improve the accuracy of the FEA and make it microstructurally aware, SEM micrographs were directly incorporated into ANSYS® to define the geometry. To do this, a SEM micrograph was first converted into a binary image using ImageJ software, following which the coordinates of the different phases in the solder joint, i.e., solder, IMC, and Cu, were obtained using a code written in MATLAB. These coordinates were then used to create the keypoints (or vertices) of the solder joint geometry in ANSYS®. The process of creating the meshed model from an original SEM image is shown in Fig. 4. Although this process merges the Cu_6Sn_5 and Cu_3Sn IMC layers into one, the efficacy of capturing the IMC layer as shown in Fig. 4b is remarkably good.

Only half of the solder joint, with greater focus on the region in the vicinity of the solder–substrate interface, was modeled, since the solder joint is symmetric about the x-direction (i.e., horizontal direction) and much of the stress variation is likely to occur at the interfaces. The geometry was discretized using eight-node quadrilateral elements (named Plane183 in ANSYS® terminology), which allowed both structural and thermal analysis to be performed. Mesh refinement was performed near the solder–IMC and IMC–substrate interfaces to achieve a clearer picture of the stress variation in these areas (Fig. 4c), where the elastic misfit is maximum, and to achieve mesh insensitivity. All materials were assumed to be elastic. Table I lists the material properties for the various components of the solder joint used in this study. In summary, the Young's moduli of the solder, IMC, and Cu were set as 50 GPa, 86 GPa, and 129 GPa,[16–18] respectively, and the Poisson's ratio for all materials was assumed to be equal to 0.3.[16–18] The thermal expansion coefficients of the solder, IMC, and Cu were set as 23×10^{-6} K^{-1}, 16×10^{-6} K^{-1}, and 17×10^{-6} K^{-1}, respectively.[16–18]

Two different sets of FEA were performed to capture the TC and TMC boundary conditions. In the case of TC, where the solder is not fixed to any fixture, the following boundary conditions were applied: (a) the initial reference temperature was set to −25°C (T_{min}) and the maximum temperature of 125°C (T_{max}) was applied on all the nodes during the heating cycle, and (b) symmetric displacement boundary conditions were applied on the top edge of the model. During TMC, since the joint was inserted into the bimetallic frame, wherein it was rigidly fixed to the frame at the top and bottom edges (Fig. 1) and a maximum shear strain of 0.128 was applied relative to T_{min}, the following boundary conditions were applied in addition to (a) and (b): (c) zero displacement at the bottom edge of the geometry, and (d) an x-displacement corresponding to strain of 0.128 and zero displacement in the y-direction at the top edge of the geometry. After these boundary conditions were applied, the model was solved using the high-displacement transient solver, and the stress distribution at different locations inside the solder joint at the highest temperature was obtained using the "plot" and "list" nodal solution option in ANSYS®.

RESULTS AND DISCUSSION

Growth of Interfacial IMC Layer

Figure 5 shows a few representative SEM images depicting the evolution of the interfacial IMC layer following 100 cycles of TC and TMC. It can be readily observed from Fig. 5 that the IMC layer was much thicker after 100 cycles of TMC compared with after the same number of cycles of TC in the same temperature range. Comparison of Fig. 5c and d also reveals that the bright Ag_3Sn precipitates inside the solder also underwent relatively faster coarsening during TMC, which is consistent with previous works on bulk solders.[7,11] This confirms the efficacy of the bimetallic frame used in this study for imposing strain.

Figure 6 shows the corresponding variation of the height of the IMC layer during TC, TMC, and IA. The initial thickness of the IMC layer was similar in all the samples exposed to the above three types of TME. Consistent with Fig. 5, Fig. 6a also reveals that the IMC thickened faster statistically in the case of TMC as compared with TC. The thickness of the IMC layer increased from 2.2 μm to almost 6.8 μm after 200 cycles of TMC, while the increase in thickness was from 2.2 μm to only 4.4 μm in the case of TC for the same number of cycles. This faster increase in the thickness of the IMC layer in the case of TMC suggests an additional driving force, most probably dependent on the strain (or stress), that accelerated the growth of the IMC layer as

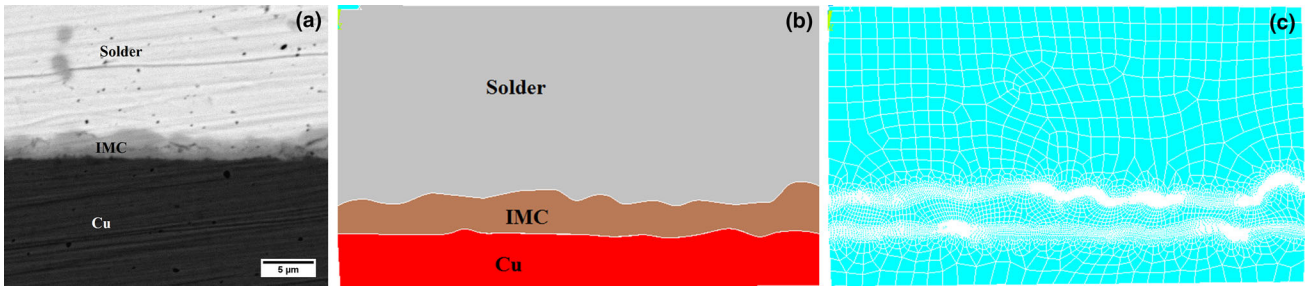

Fig. 4. (a) Original SEM micrograph, (b) corresponding geometry in ANSYS®, and (c) meshed model of a solder joint.

Table I. Values of important parameters

Parameter	Value	Ref.
Coefficient of thermal expansion (CTE) of Al	23×10^{-6} K^{-1}	15
CTE of Mo	4.8×10^{-6} K^{-1}	15
CTE of SAC solder	23×10^{-6} K^{-1}	18
CTE of Cu	17×10^{-6} K^{-1}	16
CTE of IMC	16×10^{-6} K^{-1}	17
Young's modulus of solder	50 GPa	18
Young's modulus of Cu	129 GPa	16
Young's modulus of IMC	86 GPa	17
Poisson's ratio (of all materials)	0.3	16, 17
Q_{Cu6Sn5}	81 kJ/mol	3
$D_{0,Cu6Sn5}$	5.6×10^{-8} m^2/s	3
Proportionality constant N	10^4 s	11

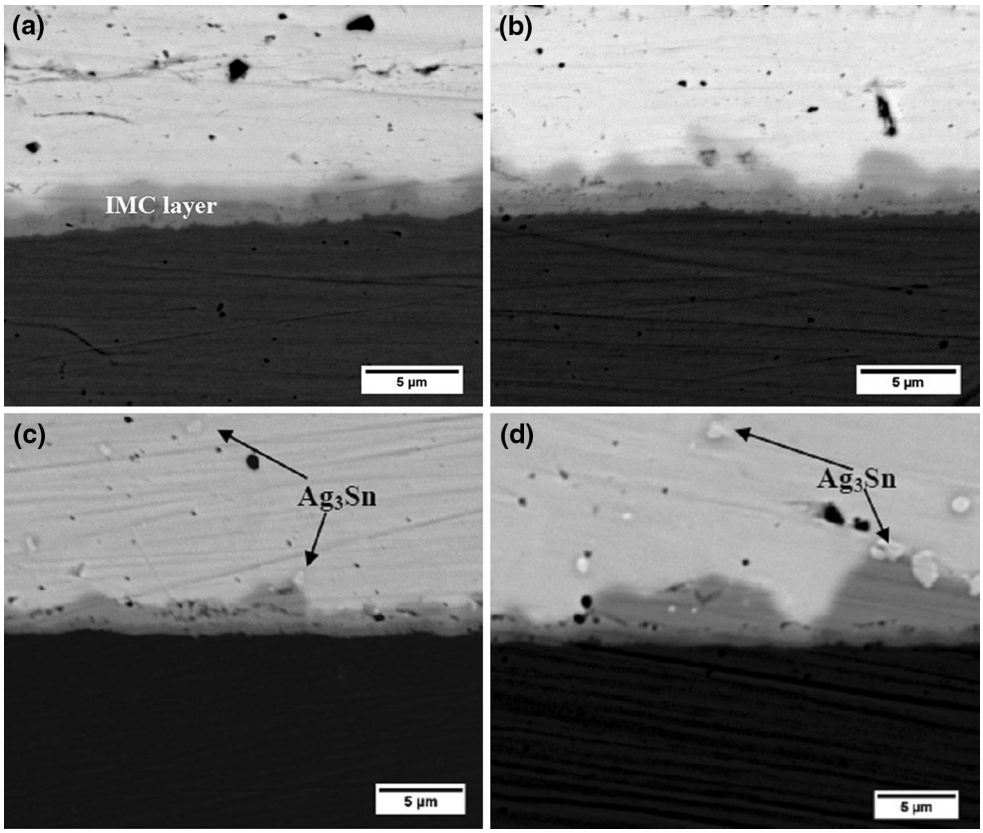

Fig. 5. Variation of morphology of interfacial IMC layer in solder-Cu joints under different types of thermomechanical excursion: (a) initial IMC in sample set for TC, (b) IMC layer after 100 cycles of TC, (c) initial IMC in the sample set for TMC, and (d) IMC after 100 cycles of TMC.

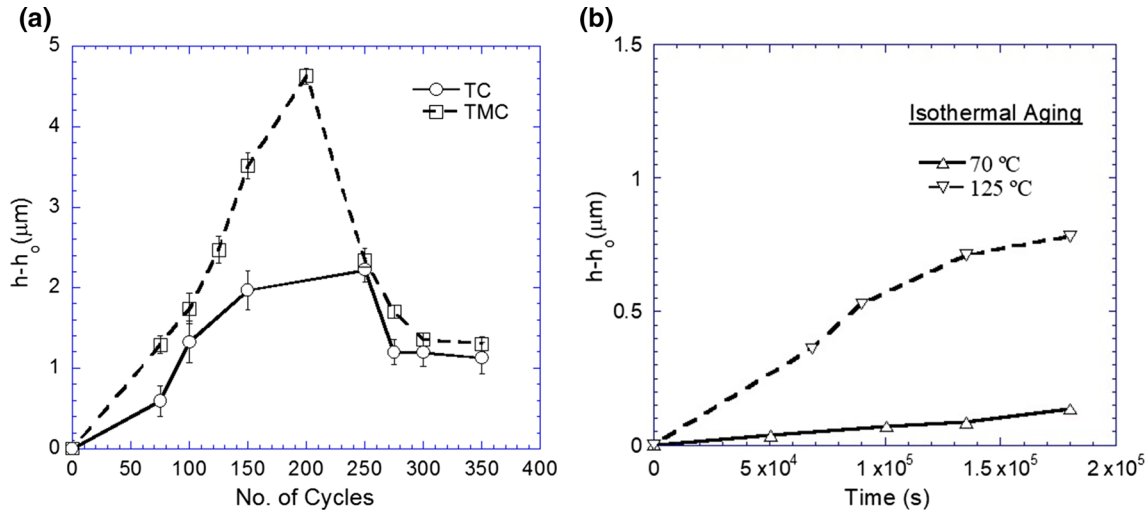

Fig. 6. Variation of thickness of interfacial IMC layer, h, during (a) TC and TMC up to 350 cycles, and (b) isothermal aging at 70°C and 125°C. h_0 is the initial thickness of the IMC layer.

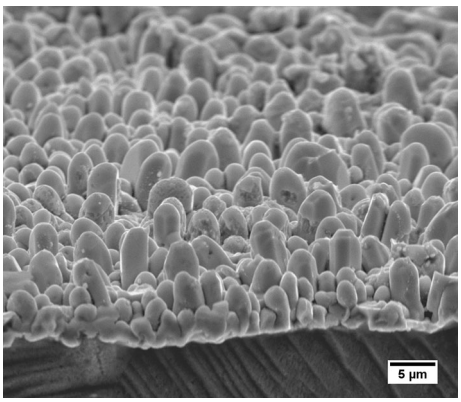

Fig. 7. Tilted view of top of Cu_6Sn_5 IMC layer obtained near the surface of the joint up to depth of ~22 μm from the surface. The solder was etched away to reveal the IMC layer.

compared with pure TC. Figure 6b shows that the increase in the IMC thickness under IA used in this study was monotonic, but less compared with TC or TMC. Also, the increase in the IMC layer thickness with time followed a similar behavior at both 70°C and 125°C; however, as expected, the growth kinetics was significantly slower at 70°C compared with 125°C.

Note that the reported increase in the height of the IMC layer during each TME will not be affected due to the surface diffusion. This is because the top 2 μm of the surface was metallographically polished every time prior to observation under SEM, which may remove the surface layer that might be noticeably affected by surface diffusion. Furthermore, the solder was selectively etched away in one of the aged samples using solution of *ortho*-nitrophenol and sodium hydroxide to reveal the top view of the IMC layer; Fig. 7 shows a slightly tilted view of the top layer. It can be readily observed in Fig. 7 that the IMC scallops grew uniformly across the joint, with no noticeable change in their size with increasing depth from the surface. In addition, the growth kinetics parameters in Eq. 1, i.e., n, Q, and D, used in this work were taken from earlier studies that measured the thickness of the IMC layer in a similar manner, i.e., by observing the growth of the IMC layer near the surface of the joint.[1–3] This ensures consistency in the adopted thickness measurement method and the growth kinetic parameters employed for analysis (in "Analytical Model for IMC Growth" section) in this study.

Figure 6a also reveals that monotonic growth of the IMC layer occurred only up to 150 to 200 cycles of both TC and TMC, beyond which the layer thickness drastically decreased to around 3.5 μm, remaining more or less constant with further thermal cycling. This observation is consistent with the behavior reported for reflowed solder joints in a previous study.[12] It should be noted that the reported values of IMC thickness are based on several SEM micrographs, so these values statistically represent the actual thickness of the IMC layer. Furthermore, Fig. 6a also shows a monotonic reduction in the IMC thickness with increase in the number of cycles beyond a certain number.

Observations similar to those in Fig. 6a, viz., a decrease in the overall thickness of the IMC layer in a diffusion couple with progression of TME, have never been reported unambiguously. However, a few studies investigating the growth kinetics of the IMC layer in miniaturized solder joints (with thickness ≤20 μm) at temperatures of 150°C and above have reported a monotonic decrease in the thickness of the Cu_6Sn_5 IMC layer after very long isothermal aging.[19–21] Herein, the overall IMC thickness (which included Cu_6Sn_5 and Cu_3Sn IMCs) either increased sluggishly or remained constant with time. In these miniature joints, the supply of Sn, which is needed for continuous growth of Cu_6Sn_5

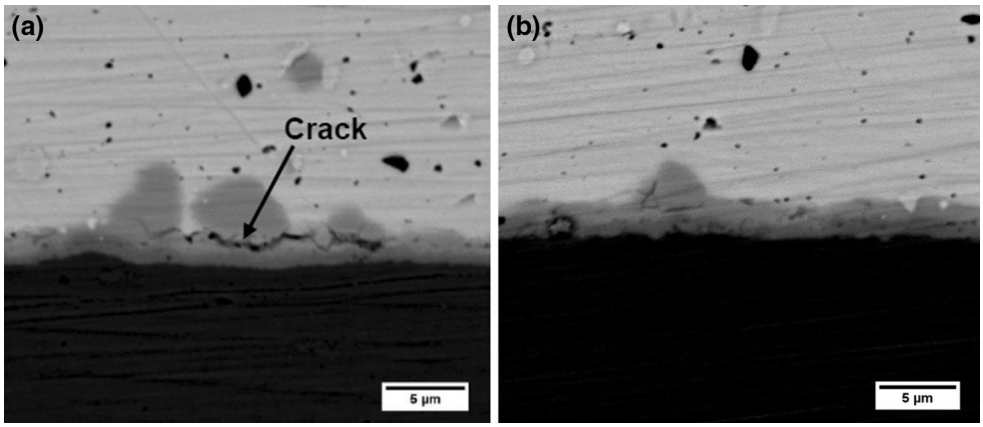

Fig. 8. Representative SEM images illustrating (a) formation of cracks in the brittle IMC layer, and (b) reduction in IMC thickness due to breaking and chipping off of the brittle IMC at higher numbers of thermal cycles.

IMC, is limited. As a result, once the Cu_6Sn_5 IMC fills the entire joint, it begins to transform into Cu_3Sn by reacting with Cu (similar to an incremental diffusion couple between Cu and Cu_6Sn_5),[19–21] thus decreasing the thickness of the Cu_6Sn-$_5$ layer. Moreover, since the reaction between Cu_6Sn_5 and Cu to form Cu_3Sn is accompanied by a decrease in specific volume of ~4.5%,[22] it may be speculated that the thickness of the overall IMC layer may also decrease upon conversion of Cu_6Sn_5 into Cu_3Sn, provided that the latter forms at a rate faster than the formation of the new Cu_6Sn_5 layer. However, since the solder joints used in this work were sufficiently thick (~1 mm), there is a negligible possibility of Cu_6Sn_5 filling the entire joint under the given TME conditions (Fig. 5).

Nevertheless, it was observed that, at higher numbers of cycles of TC as well as TMC (for example, in between 250 and 300 cycles), although the total thickness of the IMC layer reduced by ~1 μm, the thickness of the Cu_3Sn layer increased by ~0.1 μm. Hence, as explained above, there is a possibility that, as Cu_3Sn starts growing rapidly at higher numbers of cycles, the overall layer of IMCs started to contract, leading to a *real* decrease in the measurable thickness of the total IMC layer. Besides, there is also the possibility of physical cracking of the IMC layer, as shown in Fig. 8, which will lead to an apparent decrease in the thickness of the IMC layer after a very large number of cycles. Since Cu_6Sn_5 is brittle, has scallopy shape and several stress concentration points, and is subjected to strain (and hence stress)—either due to the imposed strain during TMC or TC or due to the volumetric expansion of the IMC relative to the Sn lattice saturated with Cu[23]—the entire IMC layer is prone to fracture, chipping, and cracking. Such cracks have been reported to nucleate in the IMC layer due to prolonged thermal fatigue.[2,4] As suggested in a previous study using detailed FEA simulation of solder joints under different types of TME,[12] such a decrease in the IMC layer thickness might originate from cracking and chipping of the IMC layer, which could occur due to very high stress concentration near the IMC–solder interface, especially near large sharp IMC scallops. Thus, the decrease in the height of the IMC layer could be due to either the *real* physical phenomenon of relatively faster shrinkage of the Cu_6Sn_5 layer due to the rapid growth of Cu_3Sn after a large number of cycles, or to cracking and chipping, which is an anomaly or artifact related to the testing procedure and, perhaps, metallographic polishing. It should be noted that a crack in the Cu_6Sn_5 IMC layer will essentially prevent diffusion of Cu to the Cu_6Sn_5–Sn interface as well as diffusion of Sn to the Cu_3Sn–Cu_6Sn_5 interface. This would stop further growth of Cu_6Sn_5. In this circumstance, the only IMC layer that would grow would be Cu_3Sn (and at the expense of Cu_6Sn_5). This may explain the relatively rapid increase in the thickness of Cu_3Sn as compared with Cu_6Sn_5 at very high numbers of cycles of TC and TMC.

The applicability of the former approach in the case of bulk solder joints requires further investigation of the IMC growth kinetics at higher numbers of cycles. Therefore, for the sake of simplicity in developing the model in "Analytical Model for IMC Growth" section, only the number of thermal cycles up to which monotonic growth of the IMC layer took place is considered while trying to understand the effect of stress on the growth kinetics of the IMC layer. Moreover, note that, during the initial stages of IMC growth, when the thickness increased monotonically with the severity of TME, the increase in the thickness of the Cu_3Sn layer was only 0.02 μm, being negligible compared with the growth of the Cu_6Sn_5 layer (~3.5 μm for TMC and ~2 μm for TC after 150 cycles). This implies that the growth of the IMC layer was dominated by the growth of the Cu_6Sn_5 IMC. Therefore, distinction between Cu_6Sn_5 and Cu_3Sn IMCs was not made in

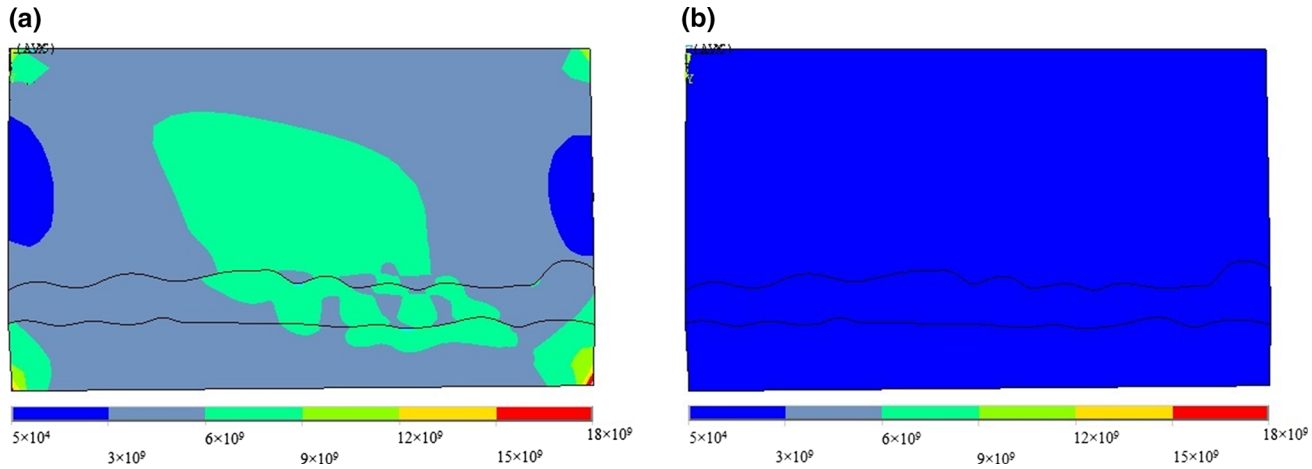

Fig. 9. Distribution of von Mises stress at different locations in the solder joint at the maximum temperature of 125°C in case of (a) thermo-mechanical cycling with shear strain of 0.128 applied on the top surface of the model and (b) thermal cycling. For ease of comparison, the range of stresses in both figures, as shown in the legend at the bottom of the figure, was kept the same.

this study, and the growth of the entire IMC layer was reasonably attributed to the growth of Cu_6Sn_5.

Microstructurally Aware Finite Element Analysis

FEA of the solder joints during thermal cycling, with and without externally imposed strain, revealed the variation of the temperature induced stress in different components of the solder joint, e.g., solder, IMC, and Cu. Figure 9 shows the distribution of von Mises stress (or effective stress) inside the solder joint at the highest temperature of 125°C under TC and TMC conditions. As shown in Fig. 9, the effective stress in the joint loaded under the TC condition at all locations, especially near the solder–IMC interface, were much lower than that in the case of TMC. This stress under the TC condition is only due to the CTE mismatch between the solder, IMC, and Cu, which is not significant, as their CTE values are similar as mentioned in "Finite Element Analysis" section and also listed in Table I. However, due to the greater strain imposed on the joint in the case of TMC, the stresses during TMC are higher than during TC. The high stress at the corners is due to the applied boundary conditions at vertices near those locations.

As shown in Fig. 9, the magnitude of the von Mises stress inside the bulk solder as well as inside the IMC layer for each condition was relatively small. However, as shown in Fig. 9a, the stress under the TMC condition was higher in the vicinity of the irregular solder–IMC interface at the center of the joint, away from the boundary. This is because the elastic mismatch between the brittle IMC and the soft solder will be maximum there, and interestingly, this effect reduces further away from the interface (or place of elastic discontinuity). In addition, the unevenness of the IMC–solder interface will also induce maximum stresses in the vicinity of the solder–IMC interface.

Analytical Model for IMC Growth

From Fig. 6, it is clearly evident that the growth kinetics of the IMC layer depends on the type of TME applied. Furthermore, as shown in Fig. 9, the stress distribution in the solder and IMC layer, which appears to affect the IMC growth kinetics, may be different in each of the three types of TME mentioned above. Besides the difference in the strain state, another major difference between the different types of TME is the applied temperature (and hence diffusion), which remains constant for the IA condition but varies continuously during TC and TMC. Due to these differences in the boundary conditions among the different types of TME, it has generally been difficult to compare the growth kinetics of the IMC layer under all three conditions on a single graph. This warrants formulation of a new single mathematical expression to explain the growth of the interfacial IMC layer by taking into account the change in temperature (and hence diffusivity) and stress (or strain) state for the different types of TME. We develop such a model below based on an earlier model developed by Dutta[24] for coarsening of Ag_3Sn (and Cu_6Sn_5) precipitates in the bulk of solders.

Assuming diffusion-controlled parabolic growth of the IMC layer,[1–3] the instantaneous growth rate at time t can be expressed as[25]

$$\frac{dh}{dt} = k_1 \frac{D}{h}, \tag{3}$$

where k_1 is a constant and D is the diffusivity, which depends on the vacancy concentration ρ_v and the activation energy for migration of atoms $Q_{m,sol}$. Diffusion of solutes occurs by sequential exchange of vacancies and solute atoms. Interestingly, the

presence of stress and the shear strain rate $\dot{\gamma}$ in the cases of TC and TMC could affect the equilibrium concentration of vacancies, ρ_v, by altering the activation energy for vacancy formation, as follows[24]:

$$\rho_v = \exp\left(-\frac{Q_{f,v} - \sigma\Omega}{RT}\right)\left[1 + N\dot{\gamma}\left[1 - \exp\left(-\frac{t}{\tau_c}\right)\right]\right], \tag{4}$$

where $Q_{f,v}$ is the activation energy for vacancy formation, σ is the stress acting in the vicinity of the atom, Ω is the atomic volume, N is a proportionality constant between the vacancy concentration and the strain rate ($\sim 10^4$ s for the TMC condition),[11] t is time, and τ_c is a time constant related to the rate of vacancy annihilation by sinks. We can assume $\tau_c \ll t$.[24] By taking into account the above considerations, the diffusivity D during temperature ramping can now be modified to include the effects of both strain rate and temperature according to the following relation:

$$D = D_0 \exp\left(-\frac{Q - \sigma\Omega}{RT}\right)(1 + N\dot{\gamma}), \tag{5}$$

where D_0 is the frequency factor and Q (= $Q_{f,v}$ + $Q_{m,sol}$) is the activation energy for diffusion.

Noting that, during TC and TMC, D changes continuously with temperature, it is necessary to define an effective value of $\overline{Dt}$ over the entire temperature cycle. Simple averaging as follows can be used to calculate $\overline{Dt}$:

$$\overline{Dt} = (\overline{Dt})_{ramp-up} + \overline{D_{T_{max}} t_{dwell}} + (\overline{Dt})_{ramp-down} + \overline{D_{T_{min}} t_{dwell}}, \tag{6}$$

where $D_{T_{max}}$ and $D_{T_{min}}$ are the diffusivities at the maximum and minimum temperature, t_{dwell} is the dwell time, and $(\overline{Dt})_{ramp-up}$ and $(\overline{Dt})_{ramp-down}$ are the diffusion distances during the ramp-up and ramp-down segments of the thermal cycle, respectively, which can be expressed as the product of the mean diffusivity over the temperature range and the diffusion time according to the following expressions:

$$(\overline{Dt})_{ramp-up} = \frac{t(1 + N\dot{\gamma})}{t_{ramp}} \int_{T_{min}}^{T_{max}} D_0 \exp\left(-\frac{Q}{RT}\right) \exp\left(\frac{\sigma_1\Omega}{RT}\right) dt, \tag{7a}$$

$$(\overline{Dt})_{ramp-down} = \frac{t(1 + N\dot{\gamma})}{t_{ramp}} \int_{T_{max}}^{T_{min}} D_0 \exp\left(-\frac{Q}{RT}\right) \exp\left(-\frac{\sigma_2\Omega}{RT}\right) dt. \tag{7b}$$

In Eq. 7, the term $t(1 + N\dot{\gamma})$ is obtained from the integration of the term involving the strain rate $\dot{\gamma}$ and time t in the expression of D as defined in Eq. 5 and represents the modified diffusion time in the presence of strain acting on the joint.

The temperature at any instant t can be given as $T = T_{min} + \beta t$, where β is the ramp rate. Combining Eqs. 7a and 7b gives the following expression for calculating $(\overline{Dt})_{both-ramps}$ for one cycle:

$$(\overline{Dt})_{both-ramps} = \frac{t(1 + N\dot{\gamma})}{t_{ramp}} \int_{T_{min}}^{T_{max}} D_0 \exp\left(-\frac{Q}{RT}\right) \left[\exp\left(\frac{\sigma_1\Omega}{RT}\right) + \exp\left(-\frac{\sigma_2\Omega}{RT}\right)\right] \frac{dT}{\beta}. \tag{8}$$

The above Eq. 8 can be further simplified by (a) assuming a symmetric temperature profile around room temperature, due to which the induced stress will be equal and opposite during the heating and cooling cycles (i.e., $\sigma_1 = \sigma_2$), (b) assuming small magnitude of stress (as Sn is a highly compliant metal), such that $\sigma\Omega/RT \ll 1$, and (c) replacing the diffusion time $t(1 + N\dot{\gamma})$ by an effective ramp time t_{eff} to capture the effect of the average strain rate $\dot{\gamma}_{avg}$ (where $\dot{\gamma}_{avg} = L\Delta\alpha\Delta T/ht_{ramp}$) acting during the temperature cycling in the case of both TC and TMC.[7,11,24] This t_{eff} accounts for the strain-enhanced diffusion of solute atoms. Making these assumptions, the effective diffusion distance of Eq. 8 can be rewritten as follows:

$$(\overline{Dt})_{both-ramps} = \frac{2t_{eff}}{t_{ramp}} \int_{T_{min}}^{T_{max}} D_0 \exp\left(-\frac{Q}{RT}\right) \frac{dT}{\beta}, \tag{9}$$

where t_{eff} is given as[7,11]

$$t_{eff} = t_{ramp}(1 + N\dot{\gamma}_{avg}). \tag{10}$$

The average strain rate, $\dot{\gamma}_{avg}$, for the TC condition is only $\sim 0.3 \times 10^{-5}$ s^{-1}, which is negligible compared with TMC, where it is $\sim 8.1 \times 10^{-5}$ s^{-1}. This small value of $\dot{\gamma}_{avg}$ under the TC condition is due to the small difference in CTE among solder, Cu, and IMC (see Table I). Therefore, for TC, one can assume $t_{eff} = t_{ramp}$, while for TMC, $t_{eff} = 1.8t_{ramp}$, suggesting that TMC was 1.8 times more effective at increasing the diffusion kinetics than TC, hence the diffusion-controlled growth kinetics of the IMC layer under TMC loading during temperature ramping increased by roughly 1.34 (i.e., $1.8^{0.5}$) times compared with TC performed under the same temperature limits. This explains the faster growth of the IMC layer during TMC as compared with TC.

Equations 8 to 10 can now be used to calculate $\overline{Dt}$ for each TME. As reported by Paul et al.,[3] the value of Q for Cu_6Sn_5 phase is ~ 81 kJ/mol, and the corresponding D_0 is $\sim 5.6 \times 10^{-8}$ m^2/s. Using these values, effective values of $\overline{Dt}$ were calculated, as

Table II. Values of effective $\overline{Dt}$ for TC, TMC, and IA at both temperatures

	$(\overline{Dt})_{ramp}$ (m^2)	$(\overline{Dt})_{T_{max}}$ at 125°C (m^2)	$(\overline{Dt})_{T_{min}}$ at −25°C (m^2)	$(\overline{Dt})_{eff}$ per Cycle (m^2)	$(\overline{Dt})_{eff}$ at End of Growth (m^2)
TC	6.7×10^{-16}	16×10^{-16}	4×10^{-22}	22×10^{-16}	3.3×10^{-13} [a]
TMC	$1.8 \times 6.7 \times 10^{-16}$	16×10^{-16}	4×10^{-22}	28×10^{-16}	4.2×10^{-13} [a]
IA at 125°C	–	–	–	–	1.8×10^{-13} [b]
IA at 70°C	–	–	–	–	3.5×10^{-15} [b]

[a]At end of 150 cycles. [b]At end of 37.5 h (equivalent to cumulative hold time at T_{max}, i.e., 125°C, after 150 thermal cycles).

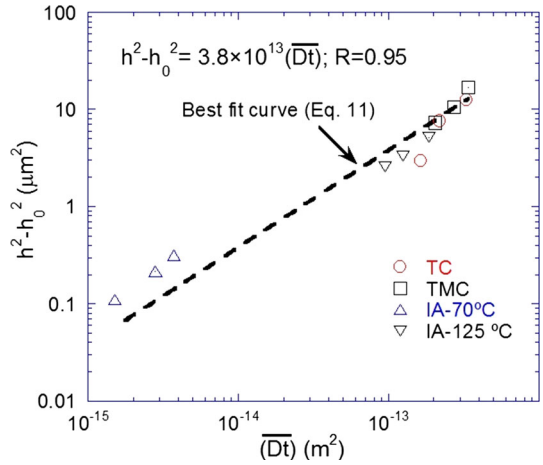

Fig. 10. Variation of thickness of IMC layer as function of $\overline{Dt}$ during various types of thermomechanical excursion. The TC and TMC data correspond only up to 150 cycles (i.e., while the thickness of the IMC increased monotonically). The broken line is the best fit curve using Eq. 11, and the legend shows the equation for the best-fit curve along with the value of the curve-fitting parameter, *R*.

listed in Table II. As confirmed by the results in Table II, the growth kinetics under the TMC condition, which recorded the highest $\overline{Dt}$, was the most severe, hence the overall growth of the IMC under the TMC condition, as shown in Fig. 6, was the highest. Furthermore, since $\overline{Dt}$ for TC was also higher compared with both IA conditions, the IMC layer grew more rapidly during TC up to 150 cycles.

In Eq. 6, the parameter $\overline{Dt}$ denotes the effective diffusion distance for each cycle such that the resultant thickness h of the IMC layer after n_c cycles is given by

$$h^2 - h_0^2 = n_c(\overline{Dt}). \tag{11}$$

In Eq. 11, the value of n_c will be equal to 1 for isothermal condition. Equation 11, which accounts for cyclic strain and variable temperature, is a suggested modification of Eq. 1 for diffusion-controlled growth of the interfacial IMC layer. Figure 10 shows the variation of the square of the thickness of the IMC layer as a function of the effective diffusion distance, $\overline{Dt}$, for solder joints exposed to all three types of TME, i.e., TC, TMC, and IA, in this study. As shown by Fig. 10, the datum points for all the types of TME lie on a single straight line with fairly good regression, thus confirming the efficacy of the developed model (i.e., Eq. 11) in capturing the growth kinetics of the interfacial IMC layer in the solder joint under an arbitrary TME.

Comparison and Validation of Developed Model Using Previously Published Data

A few previous studies have reported the growth kinetics of interfacial IMC in reflowed SAC–Cu,[26–28] SAC–Ni,[2,29] and Pb-Sn/Au-Pt-Pd[30] joints during thermal cycling (i.e., involving very small cyclic

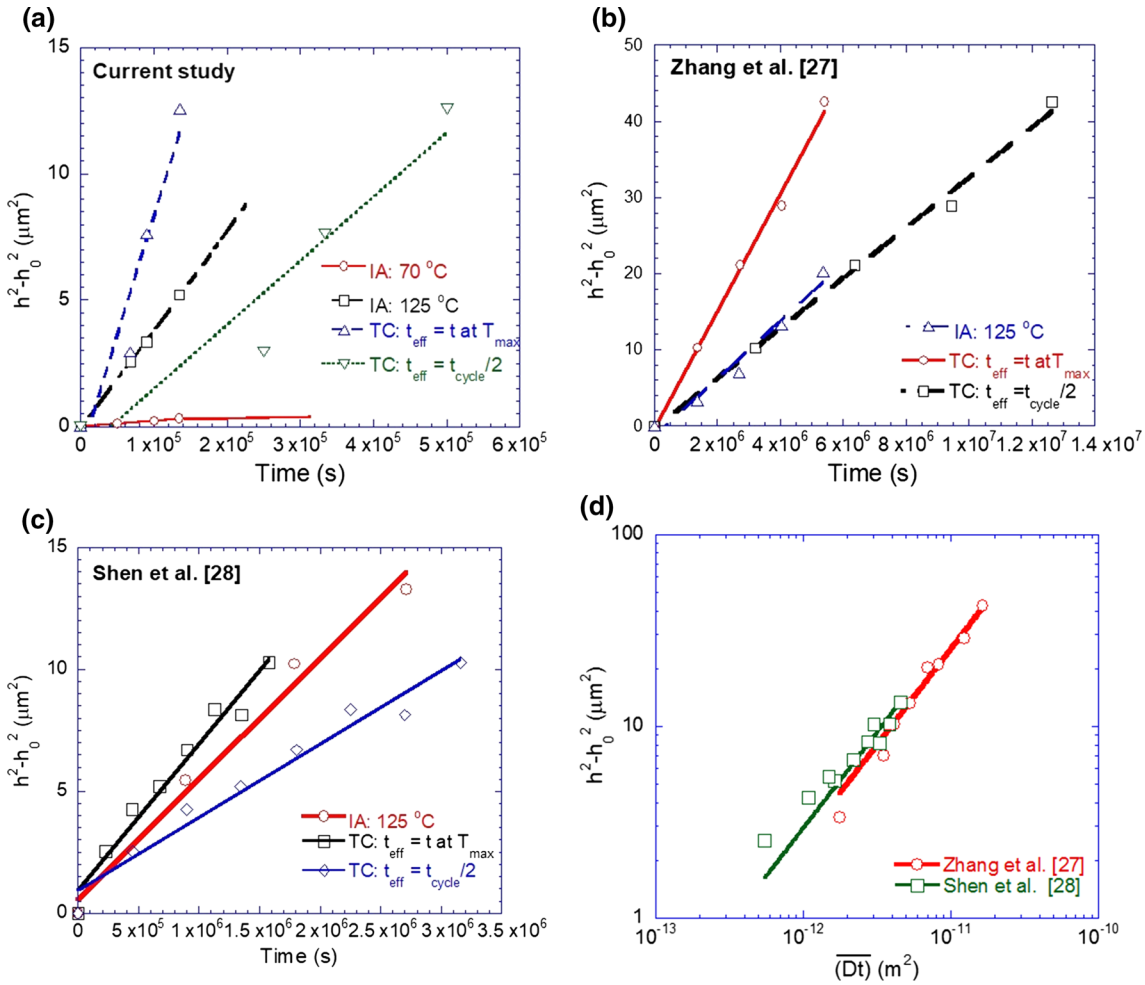

Fig. 11. Variation of IMC thickness reported in (a) present study, and by (b) Zhang et al.[27] and (c) Shen et al.[28] following the proposals of previous studies,[26–30] and (d) as a function of effective diffusion distance as proposed herein. The datum points shown in (b–d) were recalculated using the values of IMC layer thickness and time from Refs. 27 and 28.

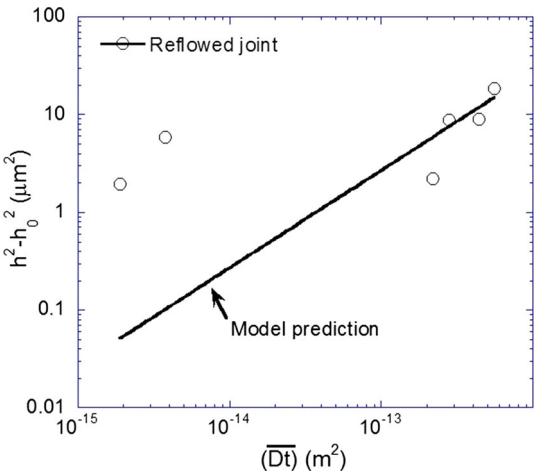

Fig. 12. Square of thickness of IMC layer in reflowed solder joints as function of effective diffusion distance for various types of TME (including IA, TC, and TMC). The solid line shows the prediction of Eq. 11.

strains owing to the small CTE mismatch between the solder and substrate) and isothermal aging. Although the temperature profiles used in those studies were similar to that considered in the present work, the ramp rates were generally much faster. Due to these higher ramp rates, limited time was available for significant diffusion to occur during temperature ramp-up and ramp-down segments. Hence, in almost all previous works, the effective diffusion time during which IMC growth occurred was approximated as the total dwell time at the maximum temperature[2,26–29] or half of the total cycle time.[31] Nevertheless, consistent with the results of this work, the above-cited studies also showed evidence of faster IMC growth kinetics under thermal cycling condition, which was attributed to thermal stresses developed in the joint during temperature cycling.[29,30]

As mentioned above, one of the objectives of this work is to develop a model that can represent the effect of various types of TME on IMC growth on a

single plot, which has been successfully achieved as described in "Analytical Model for IMC Growth" section. The model proposes a method for calculating an effective diffusion distance under the different types of TME and, subsequently, shows that the difference in the growth behavior under the various types of TME can be directly attributed to the difference in the effective diffusion distance. Now, to validate the efficacy of the developed model, we analyze previously reported data on IMC growth under TC and IA conditions using the approaches outlined in the respective studies and this work.

Figure 11 shows a set of plots of the IMC growth data under TC and IA as obtained in this work and as reported in two other studies according to the methodology reported previously: The square of the IMC layer is plotted as a function of the cumulative hold time at T_{max}, as proposed in Refs. 26 and 27, or half the total cycle time, as proposed in Ref. 30. As shown in Fig. 11a–c, the datum points obtained under IA and TC are scattered over a wide band if the methodologies proposed in Refs. 26, 27, and 30 are followed; this makes it difficult to represent the effect of these two types of TME on the IMC growth kinetics on the same graph. On the other hand, as shown in Fig. 11d, the scatter in the data is significantly minimized if the variation of the IMC layer thickness is plotted against the effective diffusion distance, i.e., according to the model developed in this work. Interestingly, Fig. 11d also shows that it is possible to represent the IMC thickness for both IA and TC on the same plot by a single straight line when using the proposed method for the previous two studies, wherein the solder joints were actually prepared using reflow method.* Thus, the model developed in this work also adequately explains the IMC growth behavior reported in other studies, performed without significant mechanical strain. Interestingly, one study indeed suggested that integration of the diffusivity over the entire range should be performed for improved accuracy[31]; however, such a methodology was not adopted in any of the previous studies.

Although the model developed in this study is suitable for diffusion-bonded solder joints, wherein the IMC layer is uniform and its growth can be assumed to be planar one-dimensional (1-D) (i.e., along its thickness), it is imperative to explore its efficacy for capturing the growth of the IMC layer in transient liquid-phase (TLP)-bonded or reflowed solder joints. It should be noted that studying the growth kinetics in TLP or reflowed solder joints will require a 2-D model, since the IMC scallops grow along both the thickness and height directions. Nevertheless, as shown in Fig. 11d, the developed model can capture the growth kinetics of the IMC layer in reflowed solder joints under IA and TC conditions, provided the IMC layer thickness is small (e.g., ~2 μm). However, as shown in Fig. 12, the same consistency is not observed for the growth kinetics of thicker IMC layers (with thickness ~4.8 μm) in reflowed solder joints growing under various types of TME. Note that the reflowed solder joints also showed similar behavior of enhanced IMC growth in presence of cyclic strain and chipping of IMC tips under TC and TMC conditions.[12] This inefficiency of the developed model in capturing the trend of IMC growth in these reflowed solder joints may be because of the large initial thickness of the IMC layer and their highly scallopy nature. If the initial thickness is large, then the growth in the vertical direction of the IMC scallops with progressive thermal cycles will be sluggish, while at the same time, the IMC scallops will continue to become wider. Thus, a 2-D model will be needed to capture the IMC growth in reflowed joints with thicker and scallopy IMC layers.

*Although the developed model is strictly valid for diffusion-bonded joints, where the assumption of 1-D diffusion may be valid, it also works well for the above-cited reflowed joints, because the initial thickness of the IMC layer was very small (~2 μm).

CONCLUSIONS

1. Various types of TME, viz., IA, TC, and TMC, were performed on SAC105–Cu solder joints to examine the growth behavior of the interfacial IMC layer. The thickness of the IMC layer increased with the progression of all three types of TME, but appeared to decrease abruptly at high numbers of cycles of TC and TMC.
2. The growth rate of the IMC layer was greater in the case of TMC compared with TC, due to an additional driving force for IMC growth in presence of strain.
3. A methodology, accounting for the increased effective time for diffusion in presence of strain, was developed. The developed model allowed not only the IMC growth kinetics under all types of TME to be plotted on a single graph, but also the IMC thickness to be expressed using a single equation.

ACKNOWLEDGEMENTS

The authors would like to acknowledge the Indian Space Research Organization (ISRO)—Indian Institute of Science (IISc) Space Technology Cell (STC) (Project No. ISTC 0367) for financial assistance. The authors also thank Professor Aloke Paul of the Indian Institute of Science, Bangalore for valuable discussion.

REFERENCES

1. P. Vianco, J. Regent, and P. Hlava, *J. Electron. Mater.* 33, 991 (2004).
2. L. Xu, and J.H.L. Pang, in *Electronic Components and Technology Conference* (2006), pp. 275–282.

3. A. Paul, C. Ghosh, and W.J. Boettinger, *Metall. Mater. Trans. A* 42A, 952 (2011).
4. K. Subramanian, *Lead-Free Solders: Materials Reliability for Electronics*, 1st ed. (Hoboken, NJ: Wiley, 2012).
5. K.N. Tu, *Acta Metall.* 21, 347 (1973).
6. I. Dutta, P. Kumar, and G. Subbarayan, *JOM* 61, 29 (2009).
7. P. Kumar, Z. Huang, S.C. Chavali, D.K. Chan, I. Dutta, G. Subbarayan, and V. Gupta, *IEEE Trans. Compon. Packag. Technol.* 2, 256 (2012).
8. A.A. El-Daly, A.E. Hammad, A. Fawzy, and D.A. Nasrallh, *Mater. Des.* 43, 40 (2013).
9. D.A. Shnawah, S.B.M. Said, M.F.M. Sabri, I.A. Badruddin, and F.X. Che, *Mater. Sci. Eng. A* 551, 160 (2012).
10. A.A. El-Daly, W.M. Desoky, T.A. Elmosalami, M.G. El-Shaarawy, and A.M. Abdraboh, *Mater. Des.* 65, 1196 (2015).
11. P. Kumar, B. Talebanpour, U. Sahaym, C.H. Wen, and I. Dutta, in *13th IEEE Itherm Conference Proceedings* (2012), pp. 880–887.
12. R. Ghosh, A. Kanjilal, and P. Kumar, *Microelectron. Reliab.* 74, 44 (2017).
13. Z. Mei, *Lead Free Solder Interconnect Reliability*, ed. D. Shangguan (New York: ASM International, 2005), p. 29.
14. K. Zeng and K.N. Tu, *Mater. Sci. Eng. R Rep* 38, 55 (2002).
15. https://en.wikipedia.org/wiki/Thermal_expansion. Accessed 6 July 2017.
16. T.T. Nguyen, D. Yu, and S.B. Park, *J. Electron. Mater.* 40, 1409 (2011).
17. http://www.metallurgy.nist.gov/mechanical_properties/roomtemp_properties.jpg-CTEofIMC. Accessed 6 July 2017.
18. http://www.topline.tv/CCGA_Material.html. Accessed 6 July 2017.
19. G. Lim, B. Kim, K. Lee, J. Kim, Y. Joo, and Y. Park, *J. Electron. Mater.* 38, 2228 (2009).
20. M. Jeong, J. Kim, B. Kwak, and Y. Park, *Microelectron. Eng.* 89, 50 (2012).
21. B. Talebanpor, Z. Huang, Z. Chen, and I. Dutta, *J. Electron. Mater.* 45, 57 (2016).
22. A. Paul and S. Divinski, *Handbook of Solid State Diffusion: Volume 2: Diffusion Analysis in Material Applications* (Elsevier, 2017).
23. W.J. Boettinger, C.E. Johnson, L.A. Bendersky, K.W. Moon, M.E. Williams, and G.R. Stafford, *Acta Mater.* 53, 5033 (2005).
24. I. Dutta, *J. Electron. Mater.* 32, 201 (2003).
25. M.A. Clarkt and T.H. Alden, *Acta Metall.* 21, 1195 (1973).
26. L. Xu, and J.H.L. Pang, in *Electronics Packaging Technology Conference* (2005), pp. 863–867.
27. L. Zhang, S.B. Xue, G. Zeng, L.L. Gao, and H. Ye, *J. Alloys Compd.* 510, 38 (2012).
28. J. Shen, M. Zhao, P. He, and Y. Pu, *J. Alloys Compd.* 574, 451 (2013).
29. J.H.L. Pang, L. Xu, X.Q. Shi, W. Zhou, and S.L. Ngoh, *J. Electron. Mater.* 33, 1219 (2004).
30. P.T. Vianco, J.J. Stephens, and J.A. Rejent, *IEEE Trans. Compon. Packag. Technol.* 20, 478 (1997).
31. L. Xu, J.H.L. Pang, K.H. Prakash, and T.H. Low, *IEEE Trans. Compon. Packag. Technol.* 28, 408 (2005).